Molecular Simulation Via Connectivity-altering Monte Carlo and Scale-jumping Methods: Application to Amorphous Polystyrene

Tim Mulder, Vagelis A. Harmandaris, Alexey V. Lyulin,* Nico F. A. van der Vegt, M. A. J. Michels

Well-equilibrated atactic-polystyrene (aPS) samples are obtained through the end-bridging Monte Carlo (EBMC) algorithm. A coarse-grained (CG) description of aPS is used; monomers are represented by two CG beads. The algorithm produces correct polymer conformations on all length scales, beyond the size of the CG beads. The code is very efficient, even though the acceptance of 0.001–0.005% is approximately 10–100 times lower than in the original EB code for PE. Systems of aPS of the order of 5000 monomers (50 chains of 100 monomers on average) can be equilibrated on all length scales within a week, in a single-processor run. The computer code is also adequate for simulations of other polymers that have the same regularity in their sequence of chemical groups and that are modeled at the same or at a coarser level of description.

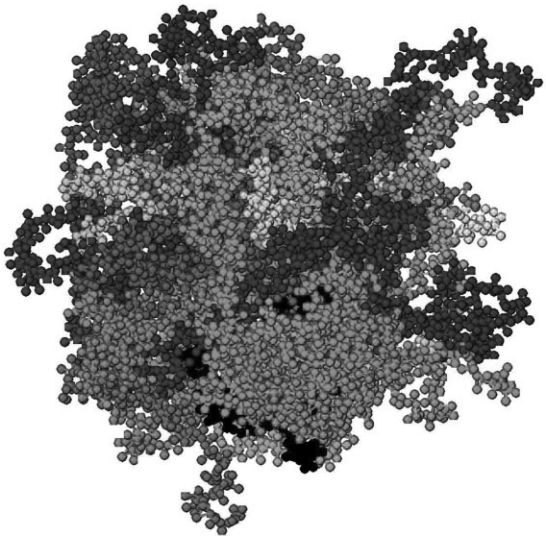

Introduction

Connectivity-altering Monte Carlo (MC) algorithms like end-bridging (EB) MC (EBMC) are very powerful tools for obtaining well-equilibrated polymer melts. EBMC was introduced in 1995[1] for equilibration of polyethylene (PE) in the melt, using a united atom-level description of a polymer. Later, it was also implemented for polypropylene (PP)[2] and polyisoprene.[3,4] The implementation of the EBMC method for any new polymer model is a very tedious job, certainly if the polymer of interest is modeled at the atomistic or united atomistic level. The change of connectivity in simulations imposed by the algorithm already asks for a lot of administration for simple polymers, such as PE, that can be modeled with one type of bead for (half a) monomer, and even more so if the polymer is more complex. So for the development of an EB code for any new polymer a huge time investment is required, and the result is only of limited use since the final algorithm can be used for one specific polymer only. Even

T. Mulder, A. V. Lyulin, M. A. J. Michels
Group Polymer Physics, Eindhoven Polymer Laboratories, Technische Universiteit Eindhoven, P.O. Box 513, 5600 MB Eindhoven, The Netherlands
E-mail: a.v.lyulin@tue.nl
T. Mulder, A. V. Lyulin, M. A. J. Michels
Dutch Polymer Institute, P.O. Box 902, 5600 AX Eindhoven, The Netherlands
V. A. Harmandaris, N. F. A. van der Vegt
Max Planck Institute for Polymer Research, Ackermannweg 10, D-55128 Mainz, Germany

DOI: 10.1002/mats.200800024

worse, one always runs the risk that the acceptance of the EB move is extremely low in case the polymer backbone is bulky and stiff, so low that hardly any moves will be accepted during the simulation. All in all, the implementation of connectivity-altering moves for polymers described at the atomistic level becomes a risky embarkment.

However, one should realize that the merit of EBMC is the possibility to equilibrate polymers on the largest length scales. Equilibration on small and intermediate length scales can also be accomplished by other techniques (by MC with more local moves, or by molecular dynamics). Because of this one could follow a two-step approach to equilibrate the polymer sample. In the first step, the sample is equilibrated on the long and intermediate length scales, i.e., at the length scales of the end-to-end distance and the length of a Kuhn segment respectively; during this step the polymer is described at a somewhat coarse-grained (CG) level and EBMC is used. To that end an existing algorithm for EBMC simulation of PE is generalized to CG polymers. In the second step, atomistic detail can be reintroduced and the sample can be equilibrated at small length scales, i.e., a few bond lengths. The advantages of this approach over the one mentioned above is that implementation of EBMC at the CG level is much easier than at a more detailed level. Furthermore, the resulting algorithm is applicable to the large class of polymers for which a CG description has a comparable functional form. A final advantage is that coarse graining will increase the acceptance probability of connectivity-altering moves.

To execute the plan sketched in the previous paragraph, one has to decide on the degree of coarse graining one prefers to use.

Figure 1 gives an overview of the various subcontinuum levels of description for polystyrene. Apart from the most detailed levels of description, being the all-atom level and the united-atom level (where all hydrogen atoms are lumped into neighboring carbon atoms) on the one hand, and the level of a freely jointed chain (consisting of segments representing Kuhn elements) on the other hand, there is the level of intermediate detail p:1 (p CG beads represent 1 monomer). The all-atom level and the united-atom level are too detailed for our purposes. The freely jointed model is too coarse to incorporate all the important chemistry-specific details. The level of p:1 coarse graining may be chosen detailed enough to distinguish different polymers and still coarse enough to make the development of connectivity-altering algorithms that can be used for many different polymers feasible. However, in this level of intermediate detail there are many possibilities. 1:1 coarse graining has been performed by Milano et al., for example for vinyl polymers.[5] Later on it has been applied as well by Vettorel et al.[6] for PE and by Spyriouni et al.[7] for polystyrene (PS). 2:1 coarse graining is performed, for example, by Tschöp et al.[8] for bisphenol-A-polycarbonate (BPAPC) and by Harmandaris et al.[9] for PS. In some cases, especially for larger monomers, with more soft degrees of freedom than for example vinyl polymers, it seems desirable to represent monomers by more than one CG particle. To prevent artifacts in the melt structure, 1:4 CG representations have been used for both BPAPC[10] and poly(ethylene terephthalate).[11]

In the present study, we are interested in obtaining well-equilibrated polymers in the bulk, especially typical glassy amorphous polymers. To that end we decided to follow the two-step equilibration procedure sketched

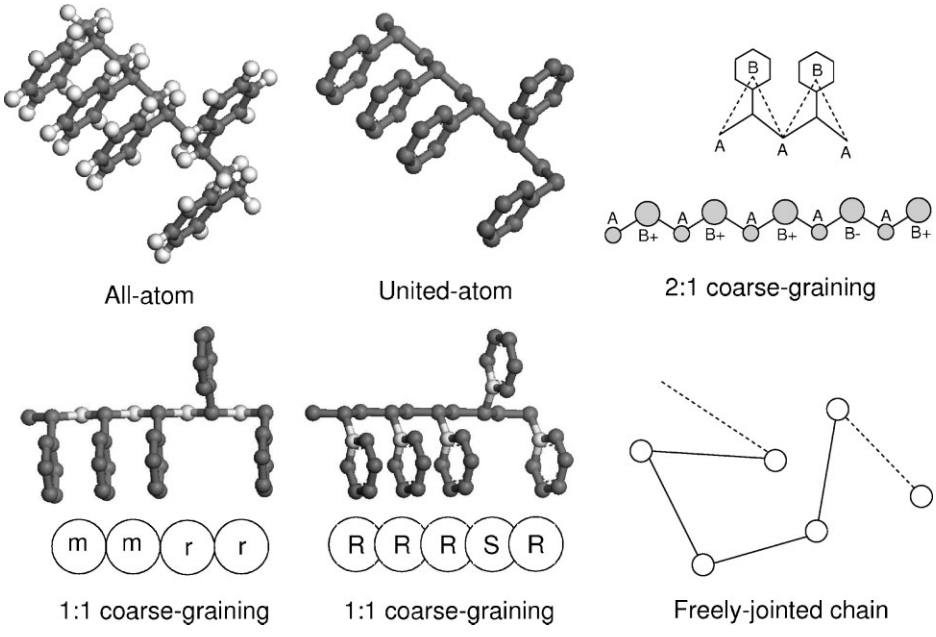

Figure 1. Overview of the various levels of description for polystyrene, from the most detailed all-atom level, via the united-atom level (where all hydrogen atoms are lumped into neighboring carbon atoms) and the more CG levels 2:1 (2 CG beads represent 1 monomer) or 1:1 (1 CG bead represents 1 monomer), to the level of a freely jointed chain consisting of beads and joints representing Kuhn segments. In the 1:1 coarse graining example, in the lower left part, the CG beads are centered at the CH_2 units; in the example in the lower part in the middle, the CG beads are centered at the C-atoms at the first positions in the phenyl rings. The symbols in the beads contain information on tacticity (*m* stands for *meso*, *r* for *racemo* dyads, *R* and *S* denote different asymmetric CHR group, other details can be found elsewhere [5]).

Macromol. Theory Simul. **2008**, *17*, 393–402

DOI: 10.1002/mats.200800024

above. To execute the first step, the level of coarse graining has been chosen that forms the best compromise between feasible implementation of EB on the one hand and not loosing structural detail on the other hand. Such a compromise has been found in the 2:1 level of coarse graining. Moreover at this level, force fields of typical glassy amorphous polymers, such as, PS and PC are available.

For equilibrating at the 2:1 level of coarse graining, an EB algorithm has been developed. An existing EBMC code for equilibration of PE in the melt has been used as the starting point. Rigorous modifications in all energy calculations and lists containing interacting particles had to be developed. Furthermore, a proper administration of alterations in the connectivity had to be set up, involving measures to prevent undesired changes in chemistry or tacticity. These tasks proved very cumbersome, justifying a generic approach that should be applicable to a whole class of polymers. After implementation, the algorithm is demonstrated for the 2:1 CG PS model developed by Harmandaris et al.[9]. The algorithm is tested on internal consistency and on performance, in terms of the CPU time needed to obtain well-equilibrated polymer melts of CG PS. The CG polymer structures resulting from simulations using the 2:1 CG PS model are used as an input for a procedure to reinsert atomistic detail.[12] In addition, the well-equilibrated atomistic configurations, resulting from the back-mapping procedure, were used for studying the deformation of atactic PS glasses in our previous publication.[13] In ref.[13] a comparison of different polymer–sample preparation and equilibration methods has been performed as well.

In the course of this project, the paper of Spyriouni et al.[7], dealing with connectivity-altering simulations of 1:1 CG PS, appeared. Spyriouni et al. were successful in preparing PS in the melt with correct global chain conformations; on the more local level, discrepancies were observed between their distributions of dyad conformations and those suggested by NMR data of Robyr et al.[14–16]. This justifies renewed attempts, such as ours, to prepare well-equilibrated PS. Comparison to the NMR data of Robyr et al.[14–16] is performed in the separate publication.[12] In general, our algorithm, which is applicable to other polymers than PS as well, is very useful when more detail than provided by 1:1 models is required.

The remainder of the paper is structured as follows. In Section 2, the generalization of the EBMC algorithm to polymers of type $(AB)_n$ and the 2:1 CG model for PS from Harmandaris et al.[9] are thoroughly explained. Subsequently, results of tests of the algorithm on dimers and oligomers are presented in Section 3. Finally, the algorithm is applied for the equilibration of long-chain polymer melts, as reported in Section 4. Conclusions are drawn in Section 5.

Coarse-grained Polymer Models and Generalization of EBMC Algorithm

In p:1 CG models, one monomer is represented by p different beads. For $p=1$, the force field controlling the motions in any degree of freedom in the CG system is rather simple. One needs bonded potentials controlling bond lengths, bond angles, and dihedrals of the polymer backbone, and non-bonded potentials to control interactions of beads in different chains or in the same chain but separated by more than (dependent on details of the model) three or four bonds (excluded-volume effects have to be taken into account properly). Clearly, with increasing p necessarily more details are included in the force field; but in addition incorporation of tacticity can add to its complexity. In the current 2:1 representation of PS tacticity information is also incorporated. In our generalization of the EBMC algorithm for PE, we take this tacticity information into account. In the remainder of this Section, the CG model that we are using is explained first (see also refs.[9,17]). Subsequently, its implementation in the EBMC algorithm is discussed.

The 2:1 Coarse-grained Model of PS

The CG mapping we use is schematically depicted in Figure 1. A-beads represent CH_2-groups on the polymer backbone, B-beads represent $CH(C_6H_5)$-groups. Tacticity is incorporated by labeling the B-beads with a + or −. After defining the direction of propagation along the chain, the tacticity label of any B-bead can be unambigiously determined as the sign of $(\vec{u}_1 \times \vec{u}_2)\,\vec{u}_p$, see Figure 2.

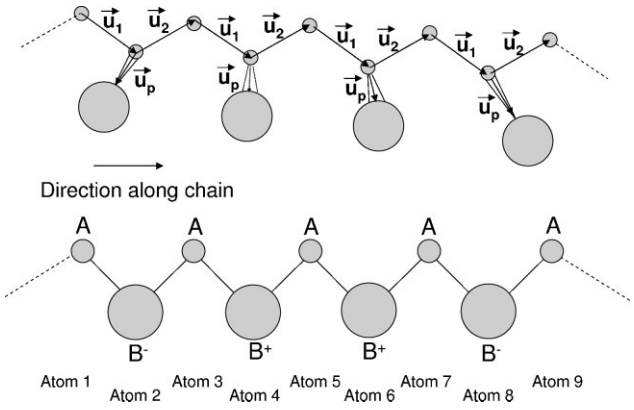

Figure 2. Elementary particles of the CG model. The upper part of the figure shows a representation of PS that is very close to the atomistic one. The small beads represent backbone atoms lumped together with hydrogens, the large particles represent phenyl rings. The lower part concerns the CG description employed in this paper. Three elementary particles are used: A for the CH_2-backbone groups, and both B^+ and B^- for $CH(C_6H_5)$-groups. The sign attached to the B contains information on tacticity.

The various bond lengths, bond angles, and dihedral angles in the CG model are controlled by force-field terms that are potentials of mean force of the CG degrees of freedom. These potentials of mean force have been obtained in atomistic simulations of isolated PS random walks, by sampling conformational distribution functions $\rho^{CG}(\{b_i\}, \{\theta_i\}, \{\phi_i\}, T)$, where $\{b_i\}$, $\{\theta_i\}$, $\{\phi_i\}$, and T represent the bond lengths, bond angles, dihedral angles, and temperature, respectively. A standard way to proceed in order to calculate the CG force fields is to assume that there exist no correlations between different degrees of freedom in the system, i.e., ρ^{CG} factorizes:

$$\rho^{CG}(\{b_i\}, \{\theta_i\}, \{\phi_i\}, T) = \prod_{i=1}^{n} \rho^{CG}(b_i, T) \prod_{i=1}^{n-1} \rho^{CG}(\theta_i, T) \prod_{i=1}^{n-2} \rho^{CG}(\phi_i, T) \quad (1)$$

The bonded potentials are obtained from inverse Boltzmann relations $U^{CG}(x,T) = -k_B T \ln \rho^{CG}(x,T)$, x being a spatial coordinate. The probability density functions $\rho^{CG}(x)$ for $x \in \{b_i\}$ and for $x \in \{\theta_i\}$ have been normalized by r_i^2 and $sin(\theta_i)$, respectively to take into account the size of volume elements. From now on T will be left out since all simulations discussed here were done at one temperature (463 K) and the notation will be ρ_x^{CG}. The distributions before normalization will be referred to as P_x^{CG} from here onwards. The factorization assumption of this specific CG mapping scheme has been thoroughly checked elsewhere.[9]

Details of the different bonded potentials are given in Table 1 and Figure 3. One type of bond length, three types of bond angles, and four types of dihedral angles are distinguished. The potentials associated with bond length and ABA bond angles can be well approximated by harmonic functions, all the other bonded potentials are numerical and are shown in Figure 3. Tacticity is incorporated in the bond angle and dihedral potentials.

In addition to the bonded interactions mentioned, there are the non-bonded interactions between CG beads in different chains and interactions between CG beads within one chain of types 1–4 and beyond, i.e., separated by at least three CG bonds. Details on these non-bonded interactions are also given in Table 1. The relevant parameters for the pair interaction of A-beads are taken from the TraPPE-UA model[18] for atactic PS, those for the pair interaction of B-beads are derived from the potential of mean force between two toluene molecules as a

Table 1. The CG PS force field from Harmandaris et al.[9] The potentials for different types of CG bond lengths, bond angles, and dihedral angles result from Boltzmann inversion of the corresponding distribution functions; the potentials associated with the bond lengths and with θ_{ABA}-type bond angles are approximated by harmonic functions. Bond angles are defined as $\theta = \pi - arccos\left(\frac{\vec{u_1}\vec{u_2}}{|u_1||u_2|}\right)$, dihedral angles ϕ are defined such that $\phi \in [0,2\pi)$ with $\phi = 0$ corresponding to the *cis* conformation and with clockwise direction of rotation. The Lennard–Jones-type potentials concern both the interactions between CG beads in different chains and the interaction between CG beads within one chain of types 1–4 and beyond, i.e., separated by at least three CG bonds.

Interaction type	Functional form	Parameters
Bond length b	$U_b = \frac{1}{2}k_b(b-l_0)^2$	$k_b = 700$ kJ·Å^{-2}·mol^{-1}, $l_0 = 3.4$ Å
Bond angles θ_{ABA}	$U_{\theta_{ABA}} = \frac{1}{2}k_{\theta_{ABA}}(\theta_{ABA}-\theta_0)^2$	$k_{\theta_{ABA}} = 5.78 \times 10^3$ kJ·rad^{-2}·mol^{-1}, $\theta_0 = 0.78$ rad
$\theta_{B^{\pm}AB^{\pm}}$	$U_{\theta_{B^{\pm}AB^{\pm}}}$	Numerical, see Figure 3
$\theta_{B^{\pm}AB^{\mp}}$	$U_{\theta_{B^{\pm}AB^{\mp}}}$	Numerical, see Figure 3
Dihedral angles		
$\phi_{AB^-AB^-}$; $\phi_{B^+AB^+A}$	$U_{\phi_{AB^-AB^-/B^+AB^+A}}$	Numerical, see Figure 3
$\phi_{B^-AB^-A}$; $\phi_{AB^+AB^+}$	$U_{\phi_{B^-AB^-A/AB^+AB^+}}$	Numerical, see Figure 3
$\phi_{AB^+AB^-}$; $\phi_{B^+AB^-A}$	$U_{\phi_{AB^+AB^-/B^+AB^-A}}$	Numerical, see Figure 3
$\phi_{AB^-AB^+}$; $\phi_{B^-AB^+A}$	$U_{\phi_{AB^-AB^+/B^-AB^+A}}$	Numerical, see Figure 3
Non-bonded		
r_{ij}, $i,j \in A,B$	$U_{LJ,ij} = 4\varepsilon_{ij}\left[\left(\frac{\sigma}{r-r_{ij}}\right)^{12} - \left(\frac{\sigma}{r-r_{ij}}\right)^{6} + \frac{1}{4}\right]$	$\sigma = 4.25$ Å, $r_{cutof\ f} = r_{ij} + 2^{1/6}\sigma$ $\varepsilon_{AA} = 0.383$ kJ·mol^{-1}, $r_{AA} = 2^{1/6}(\sigma_{AA}-\sigma)$, $\sigma_{AA} = 3.95$ Å $\varepsilon_{BB} = 3.85$ kJ·mol^{-1}, $r_{BB} = 2^{1/6}(\sigma_{BB}-\sigma)$, $\sigma_{BB} = 4.55$ Å $\varepsilon_{AB} = \sqrt{\varepsilon_{AA}\varepsilon_{BB}}$, $r_{AB} = 2^{1/6}(\sigma_{AB}-\sigma) = 0$, $\sigma_{AB} = \frac{\sigma_{AA}+\sigma_{BB}}{2}$

Macromol. Theory Simul. **2008**, *17*, 393–402

Macromolecular Journals
DOI: 10.1002/mats.200800024

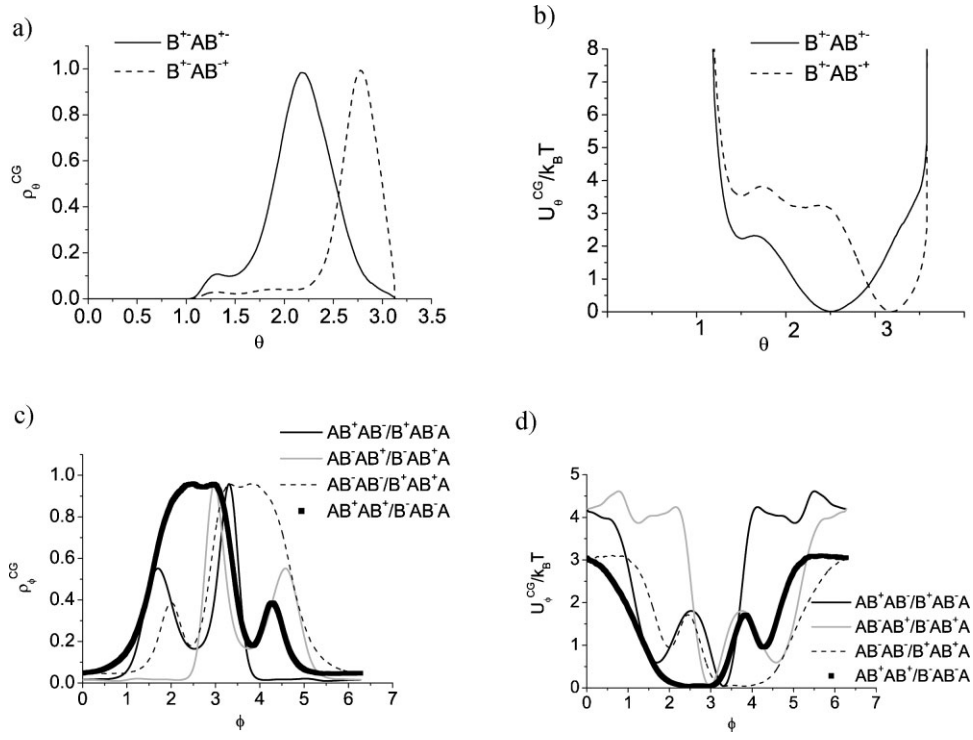

Figure 3. Distributions of CG bond angles (a) and dihedral angles (c), and the force-field components (b) and (d) obtained from these distributions using inverse Boltzmann relations. All angles are in radians.

function of the distance between them. Application of the Lorentz–Berthelot mixing rules[19] renders the parameter values of interaction of an A-bead with a B-bead: geometrical mixing ($\varepsilon_{AB} = \sqrt{\varepsilon_{AA}\varepsilon_{BB}}$) for the energy parameter and linear mixing ($\sigma_{AB} = \frac{\sigma_{AA}+\sigma_{BB}}{2}$) for the length parameter. More details about the CG force field can be found elsewhere.[9]

Generalization of EBMC for Coarse-grained Model Polymers

The starting point was an EBMC algorithm designed for and particularly efficient in equilibrating systems of PE chains of realistic molecular weight ($\overline{M}_w \gg 1$ kDa) in the melt, see ref.[1,20] All moves described there (local moves such as flips, end rotations, and concerted rotations inside the chain, and non-local moves such as reptations and end bridging moves) could be used again, although sometimes under restrictions, as explained below. The different MC moves have been used in a relative occurrence that is inversely proportional to the ratios of the numbers of particles involved in the different moves.

The force field described in Section 2.1 has been converted into tables which are read by the EBMC program. Onto the CG beads of the initial sample, type labels have been tagged (A, B^+, or B^-), in order to distinguish different kinds of beads and sequences of beads. In addition to changing the input, all routines dealing with energy calculations (or calculation of forces) have been modified. On top of this all kinds of lists used by the program have to be changed. First of all this concerns the "overlap list," which is originally created by dividing the polymer sample in some cubic cells, and allocating all atoms in the system to one of those cells. This list is used to quickly reject attempt moves that result in excluded-volume overlaps. As a complement to this list, there is a list giving for any atom the number of the cell in which it is contained. A third list is the "linked-cell list" created by dividing the system into cells of size connected to Lennard–Jones cutoff radius. The "overlap list" is now based on the largest Lennard–Jones parameter (σ_{BB}) in the force field; all atoms are allocated to cells of size $\sigma_{BB}(1+\delta)$ with $0 < \delta \ll 1$. A similar modification was needed for the "linked-cell list"; the size of the linked cell is now dictated by the range $r_{cutoff} = 2^{1/6}\sigma_{BB}$ (see Table 1) over which Lennard–Jones interactions between particles of type B (B^+ or B^-) are calculated. For many local types of moves, such as flip, end rotation, intra-chain rebridging, and volume fluctuations, this suffices.

Moves involving connectivity changes, in this case reptation and end bridging, required more measures. One point of attention is the prevention of wrong bead sequences. Reptation moves of chains with an A-bead

(B-bead) on both chain ends would result in a sequence of two A-beads (B-beads), which is undesirable and results in wrong chemistry. This could be prevented by forbidding reptation for chains with the same kind of beads on both chain ends. Alternatively one could try to reptate a whole monomer (an A- and a B-bead together). However, test runs showed that the chance of successful attempts to reptate B-beads is one to two orders of magnitude lower than the chance on successful attempts to reptate A-beads, due to the larger size of the B-beads, which give rise to larger non-bonded energy penalties for reptation. The chance of moving a whole monomer will be even lower and therefore whole-monomer reptations have not been implemented. The result of forbidding reptation for chains with the same type of beads on both chain ends results in a strongly decreased translational mobility of the chain ends for those chains; reptation of monomers as a whole results in low chain-end mobility for all chains. The consequence of this low chain-end mobility is that the efficiency of the EB move deteriorates, because of "shuttling,"[21] i.e, successive EB moves annihilating each other (moves involving the same chain end are performed forward and backward for many times). Reptation leads to considerable changes in the environment near chain ends, and with that in the candidates for performing an EB move from a particular chain end. Because of the reasons mentioned, we chose for single-atom reptation moves; to prevent undesired chemistry changes, initial samples have been prepared with exclusive chains that have different types of beads at both ends.

During EB, wrong bead sequences have been prevented by adding the criterion that beads at both sides of the trimer bridge are of the same type. Furthermore, EB moves that would result in chains with the same type of beads at both chain ends are prevented; this is necessary to prevent that subsequent reptation moves would result in undesired chemistry changes. A final issue is that in some cases the chain direction is reversed (at least for part of the chains involved in the particular EB move), see Figure 4. The B-beads for which the chain direction is reversed change from B^+ into B^- and vice versa. This required additional administration involving temporary arrays with bead-type information of attempted configurations. 50% of the MC moves were EB, the rest is divided equally between other MC moves as reptations, flips, end rotations, and concerted rotations.

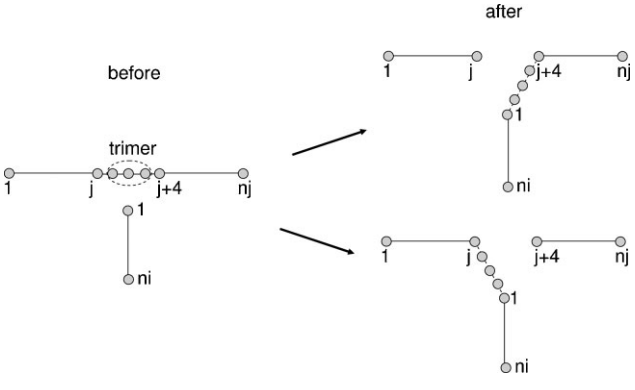

Figure 4. The EB move often results in reversion of the chain direction for part of the chain. This is the case if the final bead n_i of the attacking chain attaches to bead j in the victim chain or if the first bead of the attacking chain attaches to either bead j or bead $j+4$ of the victim chain.

Testing the Algorithm on Small Molecules

In order to test the algorithm for PS, simulations have been done first for isolated dimers in vacuum. The distributions of bond lengths, bond angles, and dihedral angles in the dimer simulations are very similar to the distributions expected based on the force field.

To test how the algorithm performs as far as more global chain properties are concerned, simulations have been done of a melt consisting of short polymer chains ($\overline{M}_w =$ 1 kDa). The distributions of bond lengths, bond angles, and dihedral angles (all not shown here) reveal slight deviations from the distributions shown in Figure 3, that have to be attributed to intra-chain interactions beyond 1–4 and to inter-chain interactions. An additional test providing insight in the chain conformations on all length scales is via the intra-chain distance distribution, giving the average square spatial distance $\langle R^2(n)\rangle$ (or $\langle R^2(N)\rangle$) between monomers in the same chain separated by n monomers (or by N CG beads) in the same chain. In Figure 5 this quantity, as obtained from the EBMC simulation mentioned, is given. $\langle R^2(n)\rangle$ is normalized by nb^2, with b the average bond length in the CG representation of PS. This normalization is convenient since for large n there should exist a proportionality between $\langle R^2(n)\rangle$ and nb^2 (Gaussian chain conformations). Also shown is the same quantity from an MD simulation of the same system.[22] The results are in close accordance.

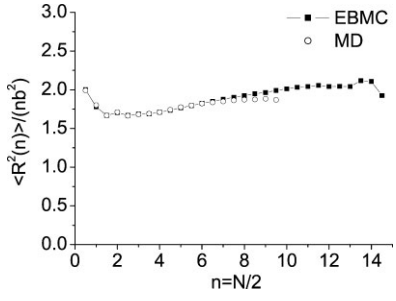

Figure 5. Distribution of intra-chain distances as obtained from simulations of short-chain polymer melts ($\overline{M}_w = 1$ kDa). Results from EBMC simulations agree well with those from MD simulations (open circles) taken from ref. [22]

Macromolecular Journals
DOI: 10.1002/mats.200800024

After performing these initial checks, the performance of the algorithm regarding the equilibration of long-chain polymer melts has been studied. The results are presented in the next Section.

Equilibration of Long-chain Polymer Melts

To study the performance of the EBMC algorithm for the equilibration of a melt ($T = 463$ K) of long PS chains, initial samples at the 2:1 level of coarse graining are prepared according to the method discussed in refs.[9,23]. In order to obtain a proper distribution of intra-chain distances, the approach described below is followed. Chains are created with a non-reversal random-walk algorithm.[23] For chains larger than 5 kDa, all chains with a non-Gaussian conformation, i.e., not satisfying

$$R^2(N) = C_\infty^{CG} N b^2 \pm 15\% \quad \text{for} \quad N > 100, \tag{2}$$

are discarded. The average bond length in the CG model is $b = 3.4$ Å. From b and the experimental value of the characteristic ratio C_∞ of polystyrene[24] it can be calculated that the characteristic ratio at the CG level C_∞^{CG} should be equal to 3.5. (C_∞ equals 8.5 at 463 K and is based on atomistic PS models: $R^2(N) = C_\infty N l^2$ with $l = 1.54$ Å.)

Subsequently the chains are arranged randomly in a simulation box, whose size is such that the density equals the experimental density[25] at the temperature studied. The resulting samples show huge local density fluctuations. In order to reduce the largest fluctuations, the samples are subjected to a zero-temperature MC simulation in which chains are only moved as rigid objects, thereby maintaining the correct distribution of intra-chain distances. In a next step MD simulations are performed, in which the non-bonded interactions are introduced slowly. As the initial distribution of intra-chain distances exhibits no overshooting at relatively small distances,[23] it can be concluded that the preparation process did not result in locally overstretched chains.

After this thorough preparation process, the sample is subjected to EBMC at a temperature of 463 K and a pressure of 1 bar, i.e., the conditions under which the 2:1 CG force field for PS had been developed. Although the initial samples are monodisperse (this is an arbitrary choice), in the EBMC run one has to allow for substantial polydispersity to make EB moves possible. The spectrum of chemical potentials, see ref.[1] is chosen such that the chain-length distribution is uniform in the interval from $\overline{X}(1-\Delta)$ to $\overline{X}(1+\Delta)$, where $\overline{X}$ is the number average degree of polymerization and Δ is the half-width of the chain length distribution reduced by the number-average chain length. The results below concern a sample of 50 chains for which $\overline{X} = 96$ ($N = 192$) and $\Delta = 0.5$. To equilibrate the sample, EB moves are combined with reptations, end rotations, flips and concerted rotations. The EB moves constitute half of the attempt moves; the other half of the attempt moves is equally distributed over all the other types of moves. No volume fluctuations are allowed, because the non-bonded interactions are purely repulsive and unlimited expansion is only temporarily prevented by topological constraints (for unentangled systems, expansion is not counteracted at all).

To judge the performance, the evolution of the internal energy has been studied, as well as the evolution of the $\overline{M}_w$-distributions (from monodisperse distribution at the start to uniform distribution between $\overline{X}(1-\Delta)$ and $\overline{X}(1+\Delta)$; also the following autocorrelation function (ACF) of the end-to-end unit vector $\vec{u} = \frac{\vec{R}_{ee}}{|\vec{R}_{ee}|}$ has been calculated:

$$\mathrm{ACF}_1(t) = \langle \vec{u}(0)\vec{u}(t) \rangle \tag{3}$$

By time t in Equation 3, we mean the number of MC Steps, MCS, where 1 MCS is the number of attempted moves divided by the total number of monomers in the system. In Figure 6 it is shown that the internal energy of the polymer sample, which is primarily related to local rearrangements, evolves to a final value within $(3–5)\times10^3$ MCS. Full decorrelation of the end-to-end unit vector $\vec{u}$, which is an indication that the sample fully lost information on its initial state, requires 1×10^4 MCS, see Figure 7. For the evolution of the $\overline{M}_w$-distribution from fully monodisperse toward uniform between $\overline{X}(1-\Delta)$ and $\overline{X}(1+\Delta)$, an equal amount of simulation time is required; the final $\overline{M}_w$-distribution is given in Figure 8, together with the theoretical perfectly uniform distribution (gray line).

The acceptance of the EB move was of the order of 0.001–0.005%, which is approximately 10–100 times lower than that in the original EBMC code,[20] developed for PE. The lower acceptance in the case of PS is primarily caused

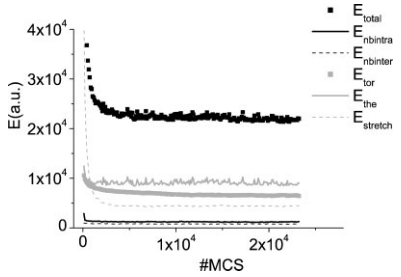

Figure 6. Internal-energy evolution, all components, i.e., the energies associated with respectively non-bonded interactions between monomers in the same chain ($E_{nb\mathrm{intra}}$) or in different chains ($E_{nb\mathrm{inter}}$), torsional angles (E_{tor}), bond angles (E_{the}), and bonds (E_{stretch}), are separated. Final values are reached within $(3–5) \times 10^3$ MC Steps, MCS, where 1 MCS is the number of attempted moves divided by the total number of monomers in the system.

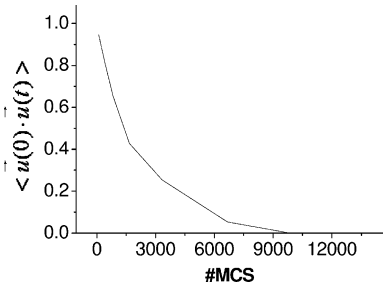

Figure 7. ACF of the end-to-end unitvector $\vec{u} = \frac{\vec{R}_{ee}}{|\vec{R}_{ee}|}$. Time t here is the number of MC steps, MCS, where 1 MCS is the number of attempted moves divided by the total number of monomers in the system.

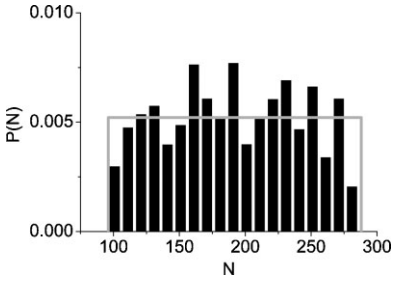

Figure 8. The distribution of chain lengths P(N) (N being the number of beads in the chain) of the simulated PS melt is in accordance with the values chosen for the chemical potentials, which prescribe a uniform distribution between $\overline{X}(1-\Delta)$ and $\overline{X}(1+\Delta)$, with $\overline{X} = 96$ ($N = 192$) and $\Delta = 0.5$. The simulations started with a monodisperse sample ($N = 192$). The final distribution of chain lengths at infinite time should be flat. The number of MCS required to obtain the final uniform distribution is of the same order as the number of steps to obtain a full decay of the ACF of the end-to-end unit vector.

by the larger excluded volume of the beads in PS than of those in PE, whereas the bridgable distance is the same for both polymers. In spite of this low acceptance, equilibrating PS polymer melts with EBMC is very feasible: the simulations reported on here have been performed in one or two week's time using one Intel Itanium 2 processor (1,3 GHz, 3 Mbyte cache) on an SGI Altix 3700 system.

It would be interesting to compare the decorrelation of end-to-end unit vectors in the present EBMC simulations to the same decorrelation in an MD simulation of an equivalent system. Possibly for short chains (<100 monomers) the difference is small. Still, because of the favorable scaling of the decorrelation time in EBMC simulations with the degree of polymerization,[20] for systems of larger chains EBMC will definitely be the technique of choice for preparing well-equilibrated PS melts.

The correctness of the final result, i.e., the final structure, is not only checked via distributions of bond lengths, bond angles, and dihedral angles, but also via the internal-distances distribution of the polymer chains and the single-chain static structure factor $S(\vec{q})$:

$$S(\vec{q}) = \frac{1}{N^2}\sum_{i=1}^{N}\sum_{j=1}^{N} exp\left(i\vec{q}\left(\vec{r}_i - \vec{r}_j\right)\right) \tag{4}$$

where $\vec{q}$ is the scattering vector, and $\vec{r}_i$ and $\vec{r}_j$ are the position vectors of beads i and j, respectively. Distributions of bond lengths and angles again show slight deviations from the distributions in Figure 3, caused by intra-chain non-bonded interactions and inter-chain interactions. The internal-distance distribution, shown in Figure 9(a), does indicate Gaussian chain conformations as it tends asymptotically to a constant value as N increases. However, it does not approach $C_\infty{}^{CG} = 3.5$, the observed value is a bit lower. This has to do with the fact that simulated chains have a finite length, whereas the value of 3.5 is reported for an infinite chain length. For example Spyriouni et al.[7] also observed that C_n approaches C_∞ only for $n \geq 300$. After rotational averaging of Equation 4 one obtains

$$S(q) = \frac{1}{N^2}\sum_{i=1}^{N}\sum_{j=1}^{N} \frac{sin(q|\vec{r}_i - \vec{r}_j|)}{q|\vec{r}_i - \vec{r}_j|} \tag{5}$$

Kratky plots of Equation 5 for chains of different length N (or, to be precise, chains with their degree of polymerization in different chain-length intervals) are given in

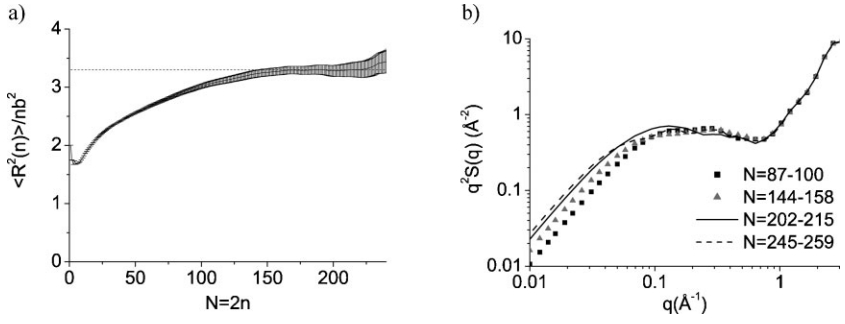

Figure 9. (a) Internal-distances distribution averaged over all chains. (b) Kratky plots for chains with their degree of polymerization in different intervals.

Macromol. Theory Simul. **2008**, *17*, 393–402

DOI: 10.1002/mats.200800024

Figure 9(b). The presence of a plateau in the curves indicates that the chain conformations are Gaussian.

All in all the EB algorithm, modified for the equilibration of polymers at the 2:1 level of description, seems adequate for the equilibration of PS melts of polymer chains with a realistic $\overline{M}_w$. Application of the algorithm to other polymers modeled at the 2:1 level of description, if necessary preceded by the development of force fields that fit the EBMC algorithm, seems a road worthwhile to pursue.

Conclusion

In order to create well-equilibrated atactic–polystyrene (aPS) samples, the so-called EBMC, a connectivity-altering MC technique, has been developed. Connectivity-altering MC techniques are very useful to equilibrate polymers on all length and time scales,[20] as the route toward well-equilibrated structures is then not dictated by the slowest relaxation processes, that is by reptation, which would be the case for instance in straightforward MD simulations.

An EBMC code had already been implemented for a PE melt, and the application of the technique to other polymers, such as PS, which is interesting in relation to the study of mechanical properties of polymers, was desirable. However, the development of an EBMC algorithm for atomistic PS proved a non-trivial task, involving a lot of bookkeeping. Moreover, in case EB is applied to polymers with bulky monomers, such as aPS, there is the risk of negligible acceptance of the EB move. By developing an algorithm for PS described at a slightly CG level, these problems have been overcome. An additional advantage is that the algorithm can be applied to other polymers that are modeled at the same or at a coarser level of description.

The EB algorithm has been developed using a 2:1-CG description of aPS developed by Harmandaris, in which every PS monomer is represented by two CG atoms, A and B, for CH_2 and $CH(C_6H_5)$, respectively. Tacticity has also been taken into account via bending- and dihedral potentials. This description is simple enough to make the development of an EB algorithm feasible. An EB algorithm for PE has been used as a starting point for the implementation of the method for PS.

Technically, the implementation meant modification of all energy calculations and related issues such as linked-cell lists (for efficient calculation of non-bonded interactions) and hard sphere overlap lists. Furthermore, measures had to be taken to prevent chemistry changes during reptation and EB moves. An additional challenge has been to deal with tacticity; for that purpose a "view direction" along the chain had to be defined and updated during EB moves. Finally, the interaction between different moves, primarily between reptation and EB had to be given special attention, both in relation to preventing changes in the chemistry and in relation to efficiency of the algorithm.

Once implemented, the code has been subjected to a number of tests. The results indicate correct implementation of the force field. All distributions of bond lengths, bond angles, and dihedral angles are in accordance with the force field. The final polymer conformations show Gaussian statistics and the value for C_∞ (the characteristic ratio based on the atomistic PS model) is approximately 8.5 at 463 K, which is in agreement with values from the literature.

The code is also very efficient, although the acceptance of the EB move is approximately 10–100 times lower than in the original EB code for PE. Systems of aPS of the order of 5000 monomers can be equilibrated on all length scales, in a single-processor run. The chain end-to-end vector orientational autocorrelations show complete decay to zero. A simulation that is started with a monodisperse mass distribution at the beginning, will evolve to an equilibrium system with a polydisperse mass distribution as dictated by the chemical potential settings. In a future publication, the well-equilibrated PS samples in the melt will be used in order to study the structural properties of this polymer cooled down to the glassy state.

Acknowledgements: This work forms part of the research program of the Dutch Polymer Institute (DPI), project 487. We acknowledge D. Theodorou for providing us the original EBMC code. Very fruitful discussions with Thomas Vettorel and Alessandra Villa are greatly appreciated.

Received: March 28, 2008; Revised: August 22, 2008; Accepted: August 22, 2008; DOI: 10.1002/mats.200800024

Keywords: coarse graining; end bridging; Monte Carlo; polystyrene

[1] P. V. K. Pant, D. N. Theodorou, *Macromolecules* **1995**, *28*, 7724.
[2] C. T. Samara, *Simulation of Polypropylene of Various Tacticities with the Monte Carlo Method*, Ph.D. Thesis. University of Patras, Patras, Greece 2000.
[3] M. Doxastakis, V. G. Mavrantzas, D. N. Theodorou, *J. Chem. Phys.* **2001**, *115*, 11339.
[4] M. Doxastakis, V. G. Mavrantzas, D. N. Theodorou, *J. Chem. Phys.* **2001**, *115*, 11352.
[5] G. Milano, F. Müller-Plathe, *J. Phys. Chem. B* **2005**, *109*, 18609.
[6] T. Vettorel, H. Meyer, *J. Chem. Theory Comput.* **2006**, *2*, 616.
[7] T. Spyriouni, C. Tzoumanekas, D. N. Theodorou, F. Müller-Plathe, G. Milano, *Macromolecules* **2007**, *40*, 3876.
[8] W. Tschop, K. Kremer, J. Batoulis, T. Bürger, O. Hahn, *Acta Polym.* **1998**, *49*, 61.

[9] [9a] V. A. Harmandaris, N. P. Adhikari, N. F. A. van der Vegt, K. Kremer, *Macromolecules* **2006**, *39*, 6708; [9b] V. A. Harmandaris, K. Kremer, arXiv:0809.1518 [cond-mat.soft].
[10] C. F. Abrams, K. Kremer, *Macromolecules* **2003**, *36*, 260.
[11] K. Kamio, K. Moorthi, D. N. Theodorou, *Macromolecules* **2007**, *40*, 710.
[12] T. Mulder, *Macromolecules*, submitted.
[13] T. Mulder, V. A. Harmandaris, A. V. Lyulin, N. F. A. van der Vegt, B. Vorselaars, M. A. J. Michels, *Macromol. Theory Simul.* **2008**, *17*, 290.
[14] P. Robyr, M. Tomaselli, C. Grob-Pisano, B. H. Meier, R. R. Ernst, U. W. Suter, *Macromolecules* **1995**, *28*, 5320.
[15] P. Robyr, Z. Gan, U. W. Suter, *Macromolecules* **1998**, *31*, 8918.
[16] P. Robyr, M. Müller, U. W. Suter, *Macromolecules* **1999**, *32*, 8681.
[17] V. A. Harmandaris, N. P. Adhikari, N. F. A. van der Vegt, K. Kremer, B. A. Mann, R. Voelkel, H. Weiss, C. C. Liew, *Macromolecules* **2007**, *40*, 7026.
[18] C. D. Wick, M. G. Martin, J. I. Siepmann, *J. Phys. Chem. B* **2000**, *104*, 8008.
[19] M. P. Allen, D. J. Tildesley, *Computer Simulation of Liquids*, Clarendon Press, Oxford 1987.
[20] V. G. Mavrantzas, T. D. Boone, E. Zervopoulou, D. N. Theodorou, *Macromolecules* **1999**, *32*, 5072.
[21] N. Ch. Karayiannis, A. E. Giannousaki, V. G. Mavrantzas, D. N. Theodorou, *J. Chem. Phys.* **2002**, *117*, 5465.
[22] V. G. Harmandaris, D. Reith, N. F. A. van der Vegt, K. Kremer, *Macrom. Chem. Phys.* **2007**, *208*, 2109.
[23] R. Auhl, R. Everaers, G. S. Grest, K. Kremer, S. J. Plimpton, *J. Chem. Phys.* **2003**, *119*, 12718.
[24] J. Mark, K. Ngai, W. Graessley, L. Mandelkern, E. Samulski, J. König, G. Wignall, *Physical Properties of Polymers*, Cambridge University Press, Cambridge, UK 2003.
[25] P. Zoller, D. J. Walsh, *Standard Pressure-Volume-Temperature Data for Polymers*, Technomic Publishing Co., Lancaster Basel 1995.

DOI: 10.1002/mats.200800024